

Modification of the plasma in the near-vicinity of Enceladus by the enveloping dust

W. M. Farrell,¹ W. S. Kurth,² R. L. Tokar,³ J.-E. Wahlund,⁴ D. A. Gurnett,² Z. Wang,² R. J. MacDowall,¹ M. W. Morooka,⁴ R. E. Johnson,⁵ and J. H. Waite Jr.⁶

Received 22 July 2010; revised 30 August 2010; accepted 31 August 2010; published 26 October 2010.

[1] The plasma near Saturn's equator is quasi-corotating, but those fluid elements entering the near-vicinity of the moon Enceladus become uniquely modified. Besides the solid body, the Moon has a surrounding dust envelop that we show herein to be detected ~ 20 Enceladus radii ($1 R_E = 252$ km) both north and south of the body. Previous reports indicate that corotating plasma slows down substantially in the near-vicinity of Enceladus. We show herein that the commencement of this plasma slow down matches closely with Cassini's entry into the dense portions of the enveloping dust in the northern hemisphere above the Moon. We also examine in detail the source of the dust about 400 km above the south polar fissures. We find that a large positive potential must exist between the south pole of the moon and the spacecraft to account for ions streaming away from the pole on connecting magnetic field lines. **Citation:** Farrell, W. M., W. S. Kurth, R. L. Tokar, J.-E. Wahlund, D. A. Gurnett, Z. Wang, R. J. MacDowall, M. W. Morooka, R. E. Johnson, and J. H. Waite Jr. (2010), Modification of the plasma in the near-vicinity of Enceladus by the enveloping dust, *Geophys. Res. Lett.*, 37, L20202, doi:10.1029/2010GL044768.

1. Introduction

[2] A major discovery of the Cassini mission was the observation of a substantial gas and particulate emission at the south pole of Saturn's moon Enceladus [Porco *et al.*, 2006; Waite *et al.*, 2006; Hansen *et al.*, 2006; Dougherty *et al.*, 2006; Spahn *et al.*, 2006]. The jets originate from fissures cutting across the polar region [Porco *et al.*, 2006] and the associated gas emission is found to have a complex chemical composition [Waite *et al.*, 2006, 2009] along with large concentrations of charged dust [Spahn *et al.*, 2006; Farrell *et al.*, 2009; M. Morooka *et al.*, Dusty plasma in the vicinity of Enceladus, submitted to *Planetary and Space Science*, 2010].

[3] The encounter studied herein, called the E3 encounter, occurred on 12 March 2008. Figure 1 shows the trajectory of

the spacecraft in an Enceladus frame of reference where +x is oriented in the direction of the moon's orbital velocity, +y is oriented towards Saturn, and +z is oriented out of the moon's orbital plane. The water plume is illustrated in Figure 1 as the purple-shaded region approximately indicating the location of highest water density. The spacecraft moved primarily southward at ~ 14 km/sec, passing near and aligned with the water jets. The Enceladus' radius is ~ 250 km and thus the entire encounter lasted on the order of 10 minutes.

[4] During this 12 March 2008 E3 encounter, Cassini's Ion and Neutral Mass Spectrometer (INMS) [Waite *et al.*, 2004] found the water concentration to be $< 10^4/\text{cm}^3$ before closest approach (CA) at 19:06:11 SCET. However, concentrations increased sharply thereafter peaking near $10^7/\text{cm}^3$ between $\sim 19:06:30$ – $19:07:00$ SCET at a location directly below the south polar fissures where gas is released (see Figure 1, right). Passing southerly at larger radial distances, INMS continued to detect plume emissions at levels $> 3 \times 10^5/\text{cm}^3$ as late as 600 seconds after CA.

2. Northern Hemisphere Plasma Slowdown

[5] We first want to focus on a period of time about 1 minute before closest approach when Cassini was in the northern hemisphere and well away (> 600 km) from the jets. During this period, INMS-measured gas densities were at levels of $< 10^4/\text{cm}^3$. It was previously noted [Farrell *et al.*, 2009] that about a minute before closest approach to the Moon, at 19:05 SCET, the upper hybrid resonance (UH) emission as detected by the Radio and Plasma Wave Science (RPWS) instrument [Gurnett *et al.*, 2004] underwent a quick and abrupt frequency downshift from 80 kHz to below 30 kHz [Farrell *et al.*, 2009]. Since the UH emission is a function of electron plasma density, it was concluded that the near-moon electron density had a clear and distinct reduction by at least 80% in the northern hemisphere region. During this same time, dust/spacecraft impacts occurred at an increasingly higher rate exceeding 10 impacts per second as detected by the RPWS system. Given the low gas density, it was concluded [Farrell *et al.*, 2009] that the northern hemisphere electron depletion was associated with dust-electron absorption. The concentration of particulates was high enough in the northern hemisphere to have an inter-dust spacing less than the plasma Debye length and as such the dust enveloping the Moon was acting collectively in reducing the electron density.

[6] Tokar *et al.* [2009] examined the nature of the plasma electrons and ions during the E3 encounter as detected by the Cassini Plasma Spectrometer (CAPS) [Young *et al.*, 2004]. They found that there was an extended region of moon-plasma interactions that included 1) a northern hemisphere region where the co-rotating plasma slows from ~ 20 km/sec

¹Solar System Exploration Division, NASA Goddard Space Flight Center, Greenbelt, Maryland, USA.

²Department of Physics and Astronomy, University of Iowa, Iowa City, Iowa, USA.

³Space Science and Applications, Los Alamos National Laboratory, Los Alamos, New Mexico, USA.

⁴Swedish Institute of Space Physics, Uppsala, Sweden.

⁵Department of Material Science and Engineering, University of Virginia, Charlottesville, Virginia, USA.

⁶Space Science and Engineering, Southwest Research Institute, San Antonio, Texas, USA.

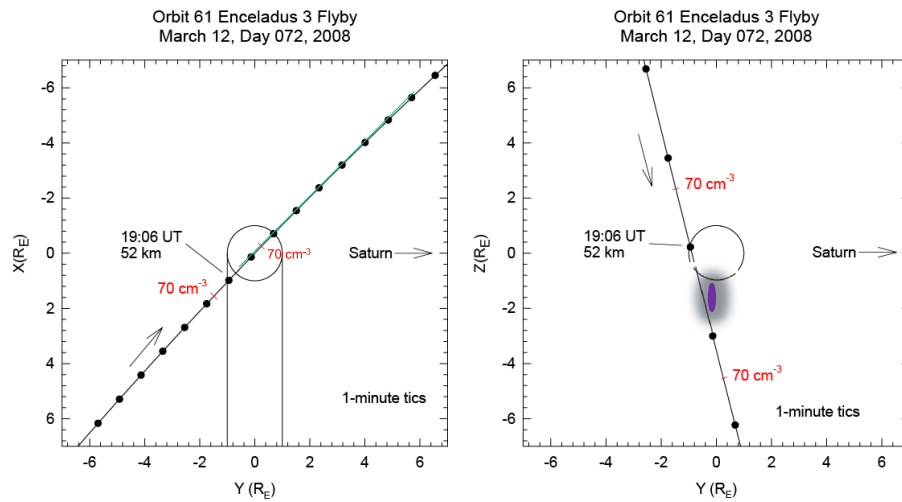


Figure 1. The Cassini trajectory during the Enceladus E3 encounter.

to near stagnation (relative to Enceladus) from 19:05:00–19:06:00 SCET, 2) a region of cold, plume ions detected between 19:06:00–19:07:00 SCET that is also decelerating to stagnation (energies consistent with the ramming speed of the spacecraft) 3) cold ion pickup after 19:06:30 SCET detected for $>8 R_E$ on the southern region below the jets and 4) a region of plasma acceleration back to pre-encounter levels between 19:07–19:08 SCET (3 to 6 R_e southward of the moon).

[7] Figure 2 shows combined plasma and plasma wave measurements from CAPS and RPWS instruments. Panel a shows the dust incident rate with the spacecraft as derived from the RPWS high frequency receiver (HFR). Bipolar voltage impulses are detected in association with dust impacts and are added (integrated) in the HFR system [Gurnett *et al.*, 1983; Kurth *et al.*, 2006; Wang *et al.*, 2006]. Shown is the overall power spectral density at 20 kHz, with power level approximately proportional to the impact rate of micron-sized grains [Wang *et al.*, 2006]. Note that dust impacts are first detected at 18:57 SCET, in northern regions nearly 20 R_E from the center of the Moon. The dust activity appears to consist of two different distributions: the first is a broad Gaussian-looking distribution with a $\sim 10 R_E$ extent about the closest approach. The second distribution appears to be a set of three distinct peaks that occur over ~ 100 seconds centered near $\sim 19:06:55$ SCET. The primary peak is in conjunction with Cassini’s transit through the jets of dust from the polar source region itself. We note that three co-incident maxima in dust impact activity were also detected in the wideband receiver, with maxima impact rates calculated at $\sim 450/\text{sec}$, $\sim 1250/\text{sec}$, and $\sim 350/\text{sec}$, respectively (Z. Wang, personal communication, 2010). Given the particle mass distribution typical of the E-ring [Kurth *et al.*, 2006; Kempf *et al.*, 2008] we infer even larger concentrations of sub-micron grains. For micron-sized grains, the grain interspacing is ~ 1.7 m while the ambient Debye length is ~ 2.5 m, thus such grains have overlapping sheaths and are acting collectively [Goertz, 1989].

[8] Figure 2b shows the northern hemisphere electron density dropout as derived from the UH emission. The electron density begins a precipitous drop-out at 19:05 SCET, about 3 R_e northward of the body center. From Langmuir

probe (LP) observations (Figure 2d), the electron density remains between 1–10% of the ion density throughout the entire interval between 19:05 and 19:08 SCET. Near 19:06:50 SCET, the ion densities peak to $3 \times 10^4 \text{ cm}^{-3}$ in the jet, but the electron-to-ion density ratio is still <0.1 . This systematic offset in electron concentration has been shown to be associated with electron absorption by small particulates, at micron and possible submicron sizes [Wahlund *et al.*, 2009; Farrell *et al.*, 2009; M. Shafiq *et al.*, Characteristics of the dust-plasma interaction near Enceladus south pole, submitted to *Planetary and Space Science*, 2010]. From Figure 2a, during this identical interval, dust impact rates continues to rise reaching over 1000 impacts per second in the jet.

[9] Figure 2c shows an ion energy spectrogram in eV/q for Anode 7 on CAPS, detecting flow in the co-rotation direction [Tokar *et al.*, 2009]. The ion activity centered near 100 eV is the corotation ion flow. This flow shows a distinct reduction in energy between 19:05–19:06:30 SCET (a slow-down in flow velocity) from 100 eV to ~ 30 eV in the northern hemisphere. The region where the plasma is slowing is indicated in Figure 2c along with the location where the flow speed increases back to pre-encounter levels near 19:08 SCET. The north hemisphere plasma deceleration is almost exactly co-aligned with the electron-dust absorption region. As indicated in Figure 2c, near and after 19:06 SCET there is also the detection of locally produced new plume ions (photo-ions, charge exchange) between 1 to 20 eV as the spacecraft moves into the concentrated gas jet region [Tokar *et al.*, 2009]. These ions initially appear at rest in the frame-of-reference of Enceladus (ram speed of Cassini), but shortly become ‘smeared’ into a broad energy band.

[10] It has been demonstrated [Goertz, 1980] that newly-formed pickup ions near a moon can act to slow the corotating plasma via local depolarization of the corotating E-field. While plasma slow down has been identified with Enceladus pickup in regions 10’s of R_E from the body [Tokar *et al.*, 2006; Pontius and Hill, 2006], Figure 2 suggests there is also slowing of the plasma due to its interaction with charged dust, especially given the temporal alignment of the northern hemisphere deceleration, electron absorption, and dust impact increases at 19:05 SCET (rather than being

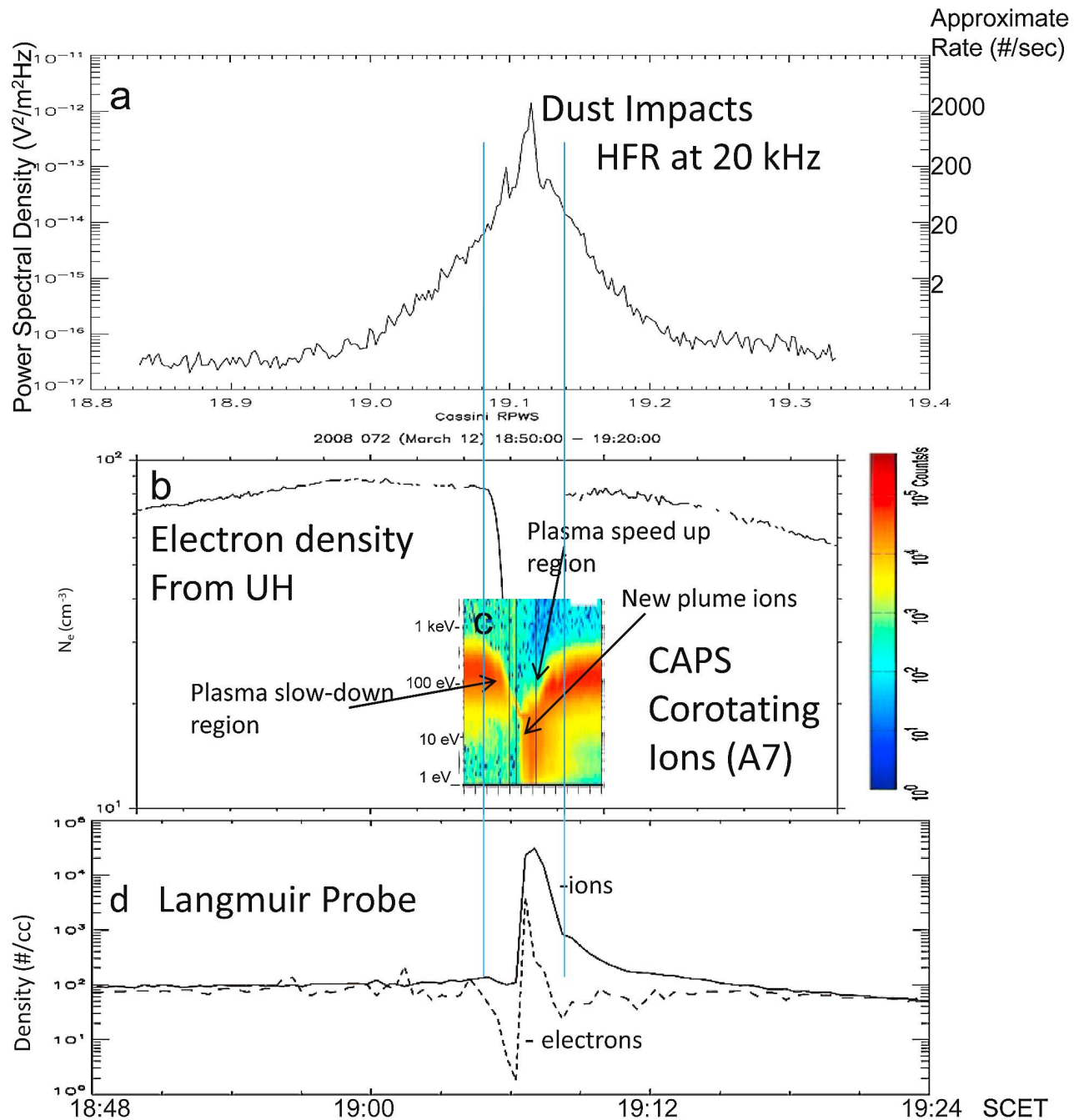


Figure 2. (a) RPWS-measured dust impact rate, (b) electron density inferred from the RPWS-measured upper hybrid emission, (c) the CAPS ion spectrometer measurements from 1 eV to 3 keV and (d) the RPWS Langmuir probe measured ion and electron densities. In Figure 2a, the impact rate assumes a comparable instrument dust response (but now scaled for the difference in intercept speed) as given by Wang *et al.* [2006].

aligned with pick-up ions detected after 19:06 SCET). Both the absorption of electrons and the deceleration of co-rotating ions appear to be coincident, each occurring over 700 km away from the densest portions of the jets. Hence, from 19:05–19:06 SCET, the slow down appears exclusively correlated with the extended dust region. Further slowdown (to stagnation) also occurs in the cold ion population possibly due to overlapping effects from ion and dust pickup, this observed between 19:06:00 to ~19:06:45 SCET.

[11] The fundamental character of the plasma changes within the collective dusty-plasma region in the north: the negative charge is now carried predominately by very massive dust grains that have absorbed the electrons, making $n_e/n_i \ll 1$. The negative charge carrier (i.e., dust) effectively become 10^{15} times more massive than the electrons and this charge carrier can move across magnetic field lines. Thus, drawing an analogy from Goertz [1980] and Pontius and Hill [2006], the negatively-charged dust grains (and their sheath

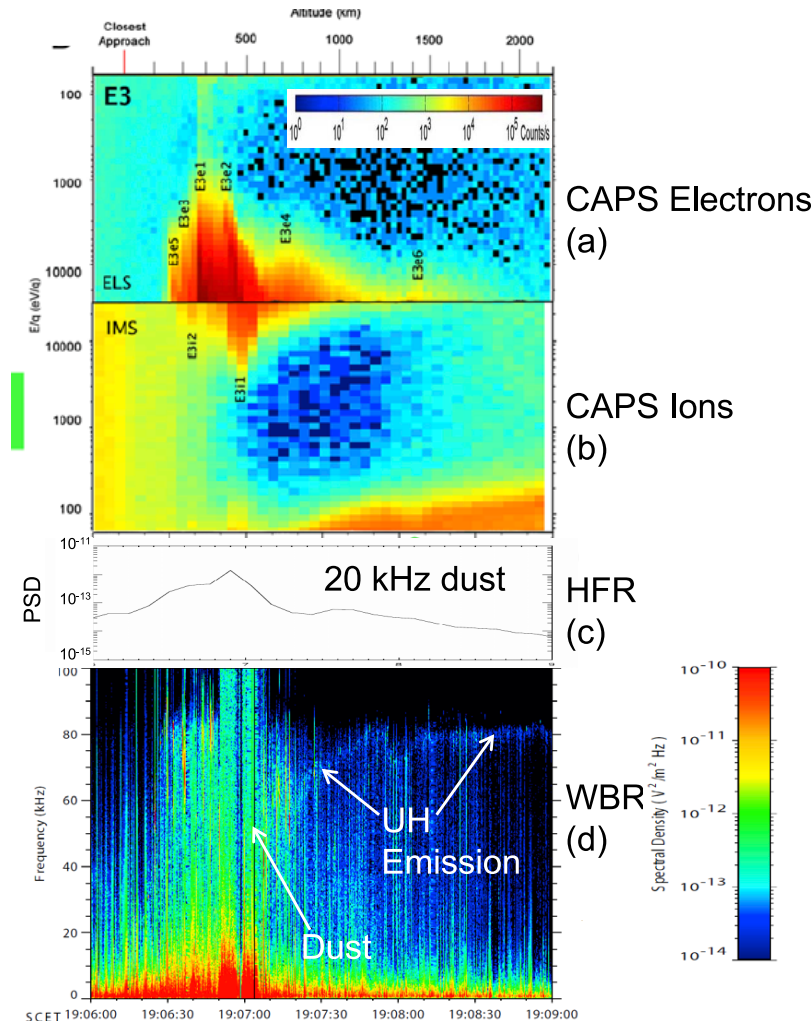


Figure 3. CAPS (a) electrons and (b) ions energy spectrogram from *Jones et al.* [2009] and RPWS (c) HFR intensity and (d) wideband receiver spectrogram during passage through the Enceladus jets. Dust impacts peak in activity near 19:06:50–19:07:10 SCET.

ions) could provide a cross-magnetic field current and perpendicular conductivity to shield the corotational E and slow down the plasma via dust mass loading processes.

3. Into the Plume

[12] Figure 3 compares a) CAPS electron and b) CAPS ion energy spectrograms [*Jones et al.*, 2009] to c) RPWS dust rate (as detected in the power spectral density in the 20 kHz high frequency receiver channel, and d) RPWS wideband waveform measurements. Panel d shows both the dust impacts (as broadband emission) and also the upper hybrid resonance emission which has a frequency that is a function of electron density, $f_{\text{uh}} = (f_{\text{pe}}^2 + f_{\text{ce}}^2)^{1/2}$ where f_{pe} is the electron plasma frequency and f_{ce} is the electron cyclotron frequency.

[13] *Jones et al.* [2009] recently suggested the compelling idea that both the CAPS ELS (electron spectrometer) and IMS (ion mass spectrometer) energetic activity above 1 keV (Figures 3a and 3b) is associated with the detection of nanoparticles in individual jets from south polar fissures. These CAPS-detected grains were presumed to be tribo-

charged by their interaction in the fissure source. In *Jones et al.*'s perspective, the CAPS ELS energetic electron signature above 1 keV (labeled as E3e1 to E3e6) is from negatively tribo-charged dust ejected from each fissure. In the CAPS IMS ion spectrogram, the activity >1 keV has also been interpreted as direct detection of positively tribo-charge dust peaking just before 19:07 SCET (labeled as E3i1 in panel b) from its fissure source.

[14] The underlying problem with this interpretation is that the initially tribo-charged grains immediately attempt to reach equilibrium with the plasma in the vicinity of the south pole region. The equilibrium time for a charged object in a plasma is $\tau \sim (kT/e) (C/|J_{\text{amb}}| A)$ [*Farrell et al.*, 2008]. For a 1 micron spherical grain of surface area $A \sim 10^{-11} \text{ m}^2$, the capacitance, C , is $\sim 10^{-16} \text{ F}$, and the environmental plasma in the jet (near 19:07 SCET as measured by the LP (Figure 2d)) has ambient current near $\sim 10^{-4} \text{ A/m}^2$ for both the electron and ion species. Thus, the dissipation time for either grain polarity is on the order of ~ 0.3 seconds for 1 micron grains, ~ 3 seconds for 0.1 micron grains, and ~ 30 seconds for 10 nm grains. For grains moving at $\sim 0.5 \text{ km/sec}$ from the fissure source, the grains acquire an equilibrium with the

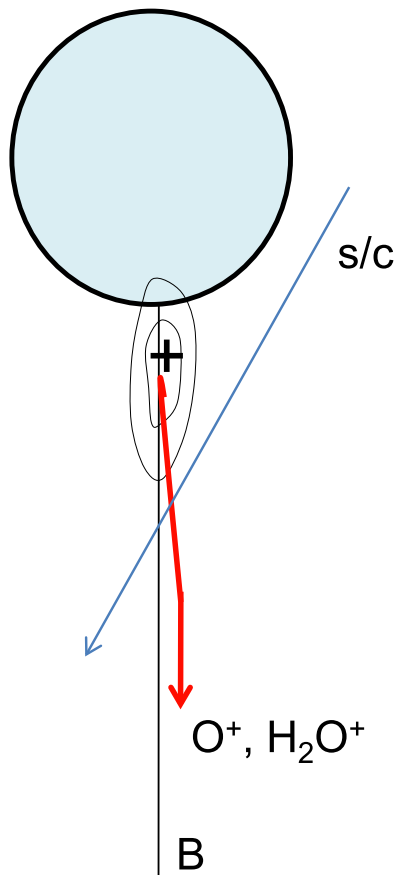


Figure 4. Illustration of the positive potential feature that exists close to Enceladus. Ions flow outward along connecting field lines in a broad range of energies that are then detected in the CAPS ram ion sensor as a highly dispersed beam having low energy (few eV) ions.

plasma in the first 10's of kilometers from Enceladus and should be in full equilibrium with the plasma by the time they are incident with Cassini at 400 km altitude. As such, it is unlikely that there is a direct detection of the initial tribocharge state for the dust grains. These grains have already been highly modified by the plasma by the time they arrive at Cassini.

[15] A comparison of the RPWS dust impacts (Figures 3c and 3d) to the CAPS observations (Figure 3b) suggests a strong overall correlation with temporal alignment of peak rates between 19:06:30–19:07:30 SCET. However, the correlation appears to break down at the 5–10 minute time scale, especially in the ELS sensor (Figure 3a). RPWS observations indicate that incident dust activity peaks at 19:06:54 SCET appearing as a single large maxima. This time corresponds to an over-flight location just after the Cairo Suicuc (19:06:52 SCET) jet passage [see Jones *et al.*, 2009, Figure 3a]. RPWS observations compares favorably to the peak in IMS activity. However, RPWS impact detections do not correlate strongly with the detailed ~5 min structure observed in the ELS sensor (presumed from nanoparticles [Jones *et al.*, 2009]). Given the fine particle susceptibility to EM forces, one might expect a nanoparticle jet to be more dispersed compared to the micron-sized dust jet sensed by RPWS. Certainly the lack of correlation at

the ~5 minute timescale suggests the need for further investigation.

[16] There is also an indication of the existence of a large positive potential located between the spacecraft at ~400 km and the polar surface (see Figure 4). The indicator for this positive potential region is the very large energy dispersion of the plume ions shown in Figure 2c [Tokar *et al.*, 2009, Figure 3b]) that extends from near 1 eV to 10's of eV after 19:06:30 SCET. Initially, newly formed ions are slowly moving at <1 km/second. However, in a positive near-moon potential, the ions should be accelerated downward (southward) along the connecting magnetic field line away from this positive potential region. The energy given to these ions is a function of their location relative to the positive potential region at the time of their photo-ion or charge-exchange birth. As such, the southern-directed beam of heavy ions should have a broad range in energy, including energies (or velocities) that are comparable to the southern-directed speed of the spacecraft at $V_{sc} \sim 10$ km/sec. In the frame of reference of the spacecraft, $v' = v - V_{sc}$, such ions moving down the field line at 10 km/sec would be detected in the A5 ram IMS detector [Tokar *et al.*, 2009, Figure 2] at very low energies (<1 eV). Progressively slower ions with $v < 10$ km/sec in the beam are rammed by the spacecraft and are thus detected at progressively higher energies in the ram-oriented sensor. The slowest ions moving down the field line at $v < 1$ km/sec are thus detected at the full spacecraft ram speed. As such, as Cassini intercepts this southward directed ion beam, it should observe a broad range of energies from <1 eV to 10's of eV. This broad ion energy spectra is indeed observed by the A5 ram and also the A7 corotating CAPS IMS sensors with the signature intensifying near 19:07 SCET [Tokar *et al.*, 2009, Figure 2] (see Figure 2c herein). The apparent smearing of ion energies below the ramming speed should only occur if the ions have been accelerated southward from their initially slow plume speeds (<1 km/s) to spacecraft velocities close to 10 km/sec—consistent with the existence of a positive potential region closer to the moon. As inferred from Jones *et al.* [2009], near-surface grain-fissure tribocharging may be one possible source for this potential.

[17] In summary, we demonstrate that the dusty environment surrounding Enceladus has a profound effect on the local plasma environment in a number of ways, including the absorption of electrons entering at the outer fringe of the moon-surrounding dust envelop, substantial slowing of the originally-corotating plasma at this dust interaction region, and the possible presence of a positive dust-related potential close to or at the moon that drives heavy ions down (southward) along the south pole connected field line.

References

- Dougherty, M. K., et al. (2006), Identification of a dynamic atmosphere at Enceladus with the Cassini magnetometer, *Science*, 311, 1406, doi:10.1126/science.1120985.
- Farrell, W. M., et al. (2008), Concerning the dissipation of electrically charged objects in the shadowed lunar polar regions, *Geophys. Res. Lett.*, 35, L19104, doi:10.1029/2008GL034785.
- Farrell, W. M., et al. (2009), Electron density dropout near Enceladus in the context of water-vapor and water-ice, *Geophys. Res. Lett.*, 36, L10203, doi:10.1029/2008GL037108.
- Goertz, C. K. (1980), Io's interaction with the plasma torus, *J. Geophys. Res.*, 85, 2949, doi:10.1029/JA085iA06p02949.
- Goertz, C. K. (1989), Dusty plasmas in the solar system, *Rev. Geophys.*, 27, 271, doi:10.1029/RG027i002p00271.

- Gurnett, D. A., et al. (1983), Micron-sized particles detected near Saturn by the Voyager plasma wave instrument, *Icarus*, *53*, 236, doi:10.1016/0019-1035(83)90145-8.
- Gurnett, D. A., et al. (2004), The Cassini radio and plasma wave investigation, *Space Sci. Rev.*, *114*, 395, doi:10.1007/s11214-004-1434-0.
- Hansen, C. J., et al. (2006), Enceladus' water vapor plume, *Science*, *311*, 1422, doi:10.1126/science.1121254.
- Jones, G. H., et al. (2009), Fine jet structure of electrically charged grains in Enceladus' plume, *Geophys. Res. Lett.*, *36*, L16204, doi:10.1029/2009GL038284.
- Kempf, S., et al. (2008), The E-ring in the vicinity of Enceladus: 1. Spatial distribution and properties of the ring particles, *Icarus*, *193*, 420, doi:10.1016/j.icarus.2007.06.027.
- Kurth, W. S., et al. (2006), Cassini RPWS observations of dust in Saturn's E ring, *Planet. Space Sci.*, *54*, 988, doi:10.1016/j.pss.2006.05.011.
- Pontius, D. H., and T. W. Hill (2006), Enceladus: A significant plasma source for Saturn's magnetosphere, *J. Geophys. Res.*, *111*, A09214, doi:10.1029/2006JA011674.
- Porco, C. C., et al. (2006), Cassini observes the active south pole of Enceladus, *Science*, *311*, 1393, doi:10.1126/science.1123013.
- Spahn, F., et al. (2006), Cassini dust measurements at Enceladus and implications for the origin of the E-ring, *Science*, *311*, 1416, doi:10.1126/science.1121375.
- Tokar, R. L., et al. (2006), The interaction of the atmosphere of Enceladus with Saturn's plasma, *Science*, *311*, 1409, doi:10.1126/science.1121061.
- Tokar, R. L., R. E. Johnson, M. F. Thomsen, R. J. Wilson, D. T. Young, F. J. Crary, A. J. Coates, G. H. Jones, and C. S. Paty (2009), Cassini detection of Enceladus' cold water-group plume ionosphere, *Geophys. Res. Lett.*, *36*, L13203, doi:10.1029/2009GL038923.
- Wahlund, J.-E., et al. (2009), Detection of dusty plasma near the E-ring of Saturn, *Planet. Space Sci.*, *57*, 1795, doi:10.1016/j.pss.2009.03.011.
- Waite, J. H., Jr., et al. (2004), The Cassini ion and neutral mass spectrometer (INMS) investigation, *Space Sci. Rev.*, *114*, 113, doi:10.1007/s11214-004-1408-2.
- Waite, J. H., Jr., et al. (2006), Cassini Ion and Neutral Mass Spectrometer: Enceladus plume composition and structure, *Science*, *311*, 1419, doi:10.1126/science.1121290.
- Waite, J. H., Jr., et al. (2009), Liquid water on Enceladus from observations of ammonia and ^{40}Ar in the plume, *Nature*, *460*, 487, doi:10.1038/nature08153.
- Wang, Z., et al. (2006), Characteristics of dust particles detected near Saturn's ring plane with the Cassini radio and plasma wave instrument, *Planet. Space Sci.*, *54*, 957, doi:10.1016/j.pss.2006.05.015.
- Young, D. T., et al. (2004), Cassini plasma spectrometer investigation, *Space Sci. Rev.*, *114*, 1, doi:10.1007/s11214-004-1406-4.

W. M. Farrell and R. J. MacDowall, Solar System Exploration Division, NASA Goddard Space Flight Center, Mail Code 695, Greenbelt, MD 20771, USA. (william.farrell@gssc.nasa.gov)

D. A. Gurnett, W. S. Kurth, and Z. Wang, Department of Physics and Astronomy, University of Iowa, Iowa City, IA 52242-1479, USA.

R. E. Johnson, Department of Material Science and Engineering, University of Virginia, Thornton Hall B103, Charlottesville, VA 22903, USA.

M. W. Morooka and J.-E. Wahlund, Swedish Institute of Space Physics, Box 537, SE-751 21 Uppsala, Sweden.

R. L. Tokar, Space Science and Applications, Los Alamos National Laboratory, Mail Stop D466, Los Alamos, NM 87545, USA.

J. H. Waite Jr., Space Science and Engineering, Southwest Research Institute, PO Drawer 28510, 6220 Culebra Rd., San Antonio, TX 78228-0510, USA.